Egyptian Journal of Petroleum (2011) **20**, 17–23

Egyptian Petroleum Research Institute

**Egyptian Journal of Petroleum**

www.elsevier.com/locate/egyjp
www.sciencedirect.com

# Formation of water-in-diesel oil nano-emulsions using high energy method and studying some of their surface active properties

**A.M. Al-Sabagh [a], Mostafa M. Emara [b], M.R. Noor El-Din [a,*], W.R. Aly [c]**

[a] *Egyptian Petroleum Research Institute (EPRI), 1 Ahmed El-Zomor St., Nasr City, Cairo 11727, Egypt*
[b] *Al-Azhar University, Faculty of Science (Men), Cairo, Egypt*
[c] *Cairo Petroleum Refining Company, Tanta, Egypt*

Available online 19 October 2011

**KEYWORDS**

Nano-emulsion;
Emulsification;
Dynamic light scattering (DLS);
Interfacial tension;
Transmission Electron Microscopy (TEM)

**Abstract** In this work, formations of water-in-diesel oil nano-emulsions using water/mixed non-ionic surfactant/diesel oil system have been studied. The high energy emulsification method was used to form three emulsions using different water contents: 5%, 10% and 14% (v/v) namely; E1, E2 and E3, respectively. These nano-emulsions were stabilized with emulsifiers having different Hydrophilic–Lipophilic Balance (HLB) namely; span 80 (HLB = 4.3), emarol 85 (HLB = 11) and their mixture (SE) with HLB = 10. The effect of water on the droplet size formation has been investigated. The interfacial tension and thermodynamic properties of the individual and emulsifiers blends have been studied. The interfacial tension ($\gamma$) measurements at 30 °C were used to determine the critical micelle concentration (CMC) and surface active properties of these emulsifiers. The water droplet sizes were measured by dynamic light scattering (DLS). From the obtained data, it was found that, mean sizes between 19.3 and 39 nm were obtained depending on the water content and concentration of blend emulsifiers (SE). Also, the results show that, the interfacial tension ($\gamma$) gives minimum value (10.85 mN/m) for SE comparing with individual emulsifier (17.13 and 12.77 mN/m) for span 80 and emarol 85, respectively. The visual inspection by TEM showed that the obtained results support the data obtained by dynamic light scattering.



* Corresponding author. Tel.: +20 222745902; fax: +20 2227727433.
E-mail address: mrned04@epri.sci.eg (M.R. Noor El-Din).



Peer review under responsibility of Egyptian Petroleum Research Institute.
doi:10.1016/j.ejpe.2011.06.005

ELSEVIER **Production and hosting by Elsevier**

## 1. Introduction

Nano-emulsions are a class of emulsions that can be transparent or translucent (droplet size range 50–200 nm) or "milky" (up to 500 nm) [1–3]. Unlike microemulsions, which are transparent and thermodynamically stable, nano-emulsions are only kinetically stable [4–6]. However, the long term physical stability of nano-emulsions (with no apparent flocculation or coalescence) makes them unique, and they are sometimes referred to as "approaching thermodynamic stability". In contrast to microemulsions, nano-emulsions are metastable and can be

diluted with water without changing the droplet size distribution [7]. Simple emulsions are classified as water-in-oil (W/O) or oil-in-water (O/W) depending on which phase constitutes the disperse phase [8]. O/W nano-emulsions with droplet diameters as low as 14 nm and high kinetic stability have been reported by Solans et al. [9]. However, W/O nano-emulsions are receiving increased attention since they were first reported by Landfester et al. recently [10]. Others have described their preparation by high-energy emulsification methods and used them in a variety of organic and inorganic polymerization reactions [11]. Depending on the preparation method, different droplet size distributions are achieved, explaining why the route of preparation can remarkably influence the emulsion stability. Due to their small droplet size, nano-emulsions may appear transparent, and Brownian motion prevents sedimentation or creaming, hence receive increased stability. The formation of emulsions with droplet size in the nanometer range (typically in the range 50–200 nm) [12], can be achieved either by high-energy emulsification methods (e.g. by high-shear stirring, high-pressure homogenizers, or ultrasound generators) [13] or by low-energy emulsification methods (e.g. phase inversion temperature (PIT)) [14]. Although high-energy emulsification methods allow great control of the droplet size and a large choice of composition, low-energy emulsification methods are interesting because they take advantage of the energy stored in the system to promote the formation of small droplets. At present, the diesel engine is still the most fuel-efficient combustion engine [15]. The general public has considerable concerns regarding the air pollution released by diesel engines, such as gaseous pollutants, particulate matter and an obnoxious odor. The pollutants that are emitted into the atmosphere from diesel engines, such as $NO_x$, HC, CO, $SO_x$, $CO_2$, PM, black smoke and others, are often transformed into other noxious materials that not only damage our ecology, but threatens human health as well [16]. One of the most efficient methods to reduce pollutant emission is to use an alternative clean fuel thereby to reduce emission quantity right at the very origin of the air pollution source. Diesel emulsion is considered one of the possible alternative fuels for curtailing the emission pollution of combustion equipment such as diesel engines and large power boilers [17,18]. Emulsion fuels are defined as emulsions of water in fuel with the typical composition of 5–20% of water, surfactant and the base fuel such as; kerosene or diesel. It is consistently proven that emulsion fuels significantly lower emissions of hydrocarbon (HC), carbon monoxide (CO), carbon dioxide ($CO_2$) and especially the hazardous NOx (Nitrous Oxides), and also particulate matters (PM). The main objective of this work is to prepare a water-in-diesel nano-emulsion fuel with different percentage of water via a high energy method (Ultraturrax homogenizer) and to study the effect of emulsifier concentrations on the stability of these emulsions. Also, interfacial tension for individual and blend emulsifiers as essential factors in the stability of nano emulsion was measured.

## 2. Experimental

### 2.1. Materials

In this study, technical grade diesel oil (Al-Tawn petroleum company, Egypt) was used as the continuous emulsion phase. The physical properties of this diesel oil are summarized in Table 1. The technical grade emulsifiers used throughout the investigation namely; sorbitan monooleate (Span 80) and poly (oxyethylene) (20) sorbitan trioleate (Emarol 85) were obtained from Sigma-Aldrech, germany and Nerol Chemicals, Italy, respectively. The water in all experiments was demineralized and doubly distilled.

### 2.2. Nano-emulsion formation

Nano-emulsions were prepared using ultraturrax homogenizer (Ultraturrax pro 200, USA) as a high energy emulsification method in two steps: firstly, preparing pre-emulsion by addition of water with different percentages (5%, 9% and 14%) to a mixture of span 80 and emarol 85 (in ratio 20:80, respectively), and diesel oil. The rate of addition was kept approximately constant with constant stirring at 800 rpm. Secondly, the prepared pre-emulsions were stirred by ultraturrax homogenizer with high speed (20000 rpm) for 2 min. All experiments were run at 30 °C.

### 2.3. Droplet size measurement

The mean droplet size of the prepared nano-emulsions was determined using dynamic light scattering (DLS) (Zetasizer Nano-ZS 90, Malvern, UK) at 30 °C.

### 2.4. Interfacial tension (IFT) for water/diesel oil interface

#### 2.4.1. Interfacial tension measurements ($\gamma$)

Different molar concentrations of span (80), emarol (85) and their mixture in ratio (1:5, respectively) namely; SE were dissolved in double distilled water and their interfacial tension was determined at 30 °C using Lecomte De Nouy tensiometer ring ''Kruss model Gmbh''. The instrument was daily regulated by bi-distilled water (conductivity $1.1 \times 10^6\ \Omega\ cm^{-1}$ at 25 °C) [19,20].

#### 2.4.2. Critical micelle concentration (CMC)

CMC of the span (80), emarol (85) and SE was determined by the method adopted by Rosen [21]. The interfacial tension–concentration isotherms (IFVC) curves were plotted for the prepared surfactants at different temperatures. The cmc values were determined from the abrupt change in the slope of IFVC curves.

#### 2.4.3. Efficiency ($PC_{20}$)

The efficiency ($PC_{20}$) was determined from SVC curves by taking the concentration ($mol/dm^3$) capable of suppressing the interfacial tension by 20 $mNm^{-1}$. The efficiency numbers have been calculated by extrapolating to $D = 20$ the linear portion of the IFVC curves [22].

**Table 1** Physical properties of diesel fuel fraction.

| Experiment | Value | Standard method |
|---|---|---|
| Colour | 2 | ASTM D-156 |
| Density at 15 °C ($gm/cm^3$) | 0.8427 | IP – 160 |
| Kinematics viscosity, at 40 °C ($mm^2/S$) | 3.268 | ASTM D 445-03 |
| Flash Point (°C) | 67 | IP 34/ASTM D93 |
| Boiling point/range (°C) | 150–300 | ASTM D-86 |
| Water content (wt.%) | Nil | ASTM D-4006-81 |

*2.4.4. Surface excess concentration ($\Gamma_{max}$)*

$\Gamma_{max}$ is a useful measure of the effectiveness of adsorption of surfactant at the liquid/air or liquid/liquid interface since it is the maximum value to which adsorption can be obtained [22]

$\Gamma_{max}$ can be calculated from Gibbs Eq. (1):

$$\Gamma_{max} = -(1/RT) \cdot (\delta\gamma/\delta \ln C) \quad (1)$$

where $\Gamma$ is called surface excess concentration (mol/cm$^2$), $T$ is absolute temperature (273 °C), $R$ universal constant ($R = 8.314$ Jmol$^{-1}$ deg$^{-1}$, and $\delta\gamma/\delta$ ln C is the surface activity (slope of IFVC curves) [23].

*2.4.5. Minimum surface area per molecule ($A_{min}$)*

$A_{min}$ is the minimum area per molecule in nm$^2$/molecule at the oil–water interface. The average area occupied by each adsorbed molecule is given by Eq. (2) [23]:

$$A_{min} = 1/(N_A \cdot \Gamma_{max}) \quad (2)$$

where $\Gamma_{max}$ is the surface excess in mol/m$^2$, and $N$ is "Avogadro's number $= 6.023 \times 10^{23}$ molecule/mol".

*2.4.6. Effectiveness $\pi_{cmc}$*

The effectiveness of adsorption or surface pressure $\pi_{cmc}$ of the surfactant was also calculated from the Eq. (3), [22]

$$\pi_{cmc} = \gamma_0 - \gamma_{cmc} \quad (3)$$

*2.4.7. Thermodynamic parameters of micellization*

The ability for micellization processes depends on thermodynamic parameter (Standard free energy, $\Delta G_{mic}$). Most information on the free energy of micellization has been obtained indirectly through the CMC. The $\Delta G_{mic}$ was be calculated by choosing the following expression (Eq. (4)), for the standard initial state of the non-micellar surfactant species a hypothetical state at unit mole fraction $X$, with the individual ions or molecules behaving as at infinite dilution, and for the standard final state, the micelle itself [24]

$$\Delta G_{mic} = 2.3RT(1 - \alpha) \log \text{cmc} \quad (4)$$

where $R$, the universal gas constant ($R = 3.418$ J/mol K), $T$, the absolute temperature ($T = t + 273$), and $\alpha$, the fraction of counter ions bound by micelle in case of ionic surfactants ($\alpha = 0$ for nonionic surfactants), and cmc, critical micelle concentration in g/mol.

*2.4.8. Thermodynamic parameters of adsorption*

Many investigators dealt with the thermodynamics of surfactant adsorption at interface. The thermodynamic parameter value of adsorption $\Delta G_{ad}$ were calculated via the following Eq. (5) [25]:

$$\Delta G_{ad} = \Delta G_{mic} - 0.6.23\pi_{cmc}A_{min} \quad (5)$$

## 3. Results and discussion

### 3.1. Nano-emulsion stability

The w/o nano-emulsions prepared in this work exhibited good stability without phase separation during two weeks but with a slight increase in the mean droplet size with time. The two common probable breakdown processes in these systems are coalescence and/or Ostwald ripening [26]. If coalescence was the driving force for emulsion instability, changes in droplet size with time are described by the following equation [27]

$$1/r^2 = 1/r_o^2 - 8\pi/3\omega t \quad (6)$$

where $r$ is the average droplet radius at time $t$, $r_o$ is the initial droplet radius, and $\omega$ is the frequency of rupture per the droplet surface area [28].

The said equation is used generally for the concentrated systems, but it may be utilized to show whether coalescence was the driving force for the instability. Another alternative mechanism that explains the instability of nano-emulsions is Ostwald ripening which arises from the difference in solubility between droplets with different sizes. In this process, larger droplets grow at the expense of smaller ones due to the molecular diffusion through the continuous phase. The Lifshitz -Slezov and Wagner (LSW) theory [29,30] gives an expression for the Ostwald ripening rate ($\acute{\omega}$) as shown by the equation:

$$\acute{\omega} = dr^3/dt = 8/9[(C_\infty \gamma V_m D)/dRT] \quad (7)$$

where $r$ is the average radius of droplet, $t$ is the storage time, $C_\infty$ is the solubility of the dispersed phase in the continuous phase, $\gamma$ is the interfacial tension between the dispersed phase and medium, $V_m$ is the molar volume of the dispersed phase, $D$ is the diffusion coefficient of the dispersed phase in the continuous phase, $d$ is the density of the oil (hexane), $R$ is the gas constant and $T$ is the absolute temperature. A stable nano-emulsion should have a small mean droplet size and a large Ostwald ripening coefficient.

Eq. (7) implies a linear relationship between the cube of the radius ($r^3$) and time ($t$). By plotting the $r^3$ of nano-emulsions with different surfactant concentrations as a function of time ($t$) as shown in Figs. 1 and 2, it was found that good linear plots between ($r^3$) and ($t$). Ostwald ripening rate can be calculated from the slope of each straight line. The initial and final droplet size, and Ostwald ripening rate of the prepared nano-emulsions are shown in Table 2 and illustrated in Figs. 3 and 4. Highly transparent nano-emulsion with initial droplet size (19.3 nm) was obtained at 8% emulsifier concentration and 5% water content. This droplet size value increases slightly till up to 67.2 nm after 360 h at the same condition. This may be attributed to instability of nanodroplets, where the smaller one

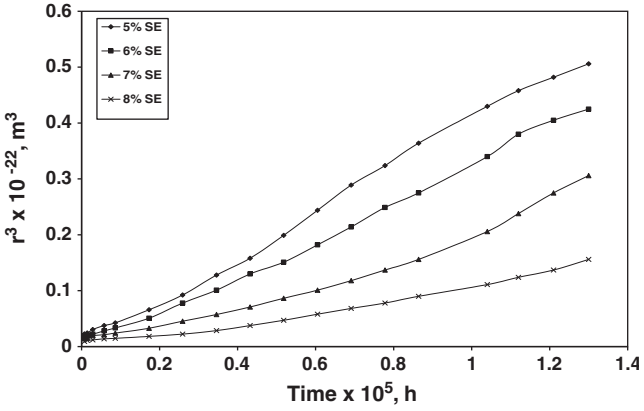


**Figure 1** Nano-emulsion $r^3$ as a function of time in system water/SE/diesel oil at 5% water content, HLB = 10, different concentration of SE and 30 °C.

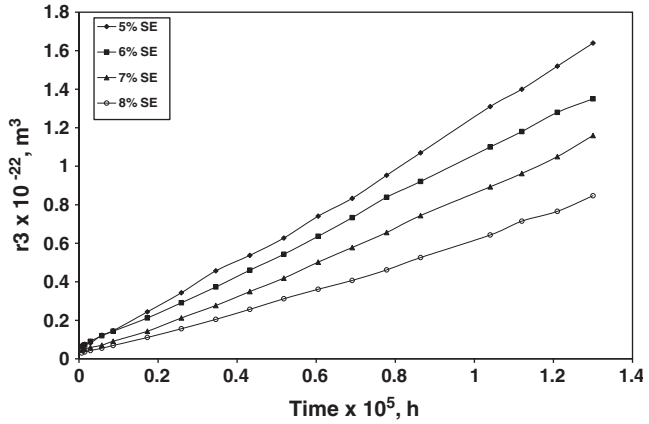


**Figure 2** Nano-emulsion $r^3$ as a function of time in system water/SE/diesel oil at 14% water content, HLB = 10, different concentration of SE and 30 °C.

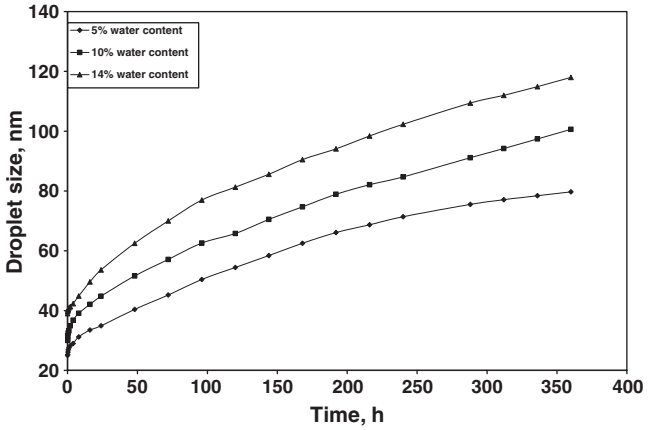


**Figure 3** Water droplet size vs. time in system water/SE/diesel oil at 5% SE, HLB = 10 and 30 °C.

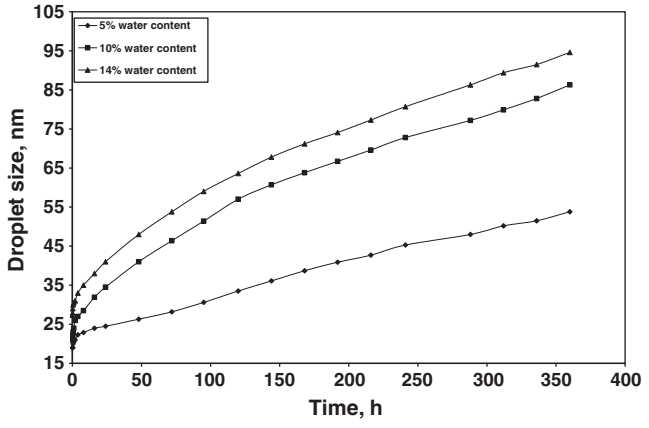


**Figure 4** Water droplet size vs. time in system water/SE/diesel oil at 8% SE, HLB = 10 and 30 °C.

of water nanodroplets will disappear by immigration to large droplets via the continuous phase [24].

Accordingly, the droplet size of these prepared nano-emulsions increased with time. Therefore, the kinetics of nano-emulsion stabilization may be attributed to Ostwald ripening (i.e., diffusion of water droplet from small to the big droplets). As mentioned before, the Ostwald ripening rate ($\acute{\omega}$)**,** is direct proportional to emulsifier concentration e.g., the Ostwald ripening rate increases with increasing of the emulsifier concentration from 5% to 8%.

**Table 2** Effect of blend emulsifiers concentration on the initial radius ($r_o$) and Ostwald ripening rate ($\acute{\omega}$) for water in diesel nano emulsion at different water content, and surfactant concentrations at 30 °C.

| SE concentration | Water content (wt.%) | $r_o$ (nm) | $\acute{\omega}$ ($m^3\ s^{-1} \times 10^{21}$) |
|---|---|---|---|
| 5% | 5 | 25 | 0.394 |
| | 10 | 30 | 0.728 |
| | 14 | 39 | 1.208 |
| 6% | 5 | 23.1 | 0.322 |
| | 10 | 27.2 | 0.654 |
| | 14 | 34.9 | 1.005 |
| 7% | 5 | 22 | 0.208 |
| | 10 | 25 | 0.628 |
| | 14 | 31 | 0.850 |
| 8% | 5 | 19.3 | 0.108 |
| | 10 | 21 | 0.462 |
| | 14 | 27.3 | 0.616 |

### *3.2. Effect of emulsifier concentration*

The emulsifier plays a major role in the formation of nano-emulsions. The high energy required for their formation can be understood from a consideration of the Laplace pressure ($P$)

$$P = 2\gamma/R \tag{8}$$

where $R$ is the radii of curvature and emulsion drop, which has to be overcome to break up a drop into smaller ones. Additional processes occur during emulsification, such as adsorption of surfactants and droplet collision, which may or may not lead to coalescence [1].

Concerning Ostawald repining rates ($\acute{\omega}$), it is clear from Figs. 1 and 2 and Table 2 that $\acute{\omega}$ decreases with increasing of surfactant concentration (from 3.943 to $1.082 \times 10^{21}$ $m^3\ s^{-1}$) at 5% water content. This phenomenon is opposite to most results reported in the literature [31]. The decrease in the Ostawald repining rates ($\acute{\omega}$) with increase the emulsifier concentration was discussed in the following items [32]:

1. The diffusion coefficient of micelles decreases as their concentration increases, because crowding effects can increase the viscosity.
2. The decrease in the average droplet size.
3. It is possible that association colloids other than micelles are formed at relatively high emulsifier concentrations
4. It is possible that the emulsifiers form thick multi-layers around the emulsion droplets, which retard the movement of the water molecules from the droplets to the surrounding aqueous phase.
5. Preliminary aggregates formed at low emulsifiers concentration are loosely associated and likely to be slightly interacting with water molecules.

### 3.3. Effect of water content on nano-emulsions droplet size

The water droplet size (nm) against the time in system water/SE/diesel oil at different emulsifier concentrations (5, and 8 wt.%) and 30 °C are shown in Figs. 3 and 4, respectively. From these figures, it is obvious that the droplet size (nm) increases with increasing of the water content (5, 10 and 14 wt.%). With increasing of the water content from 5, 10 to 14 wt.% at 8% emulsifier concentration and 30 °C, W/O nano-emulsion with mean droplet size 19.3, 27.9 and 34 nm, respectively, were obtained after 360 h and realized by increasing addition of the dispersed water phase. When the concentration of dispersed phase (water concentration) increases in the emulsion, the droplet sizes of water increases and possibly the interfacial film thickness decreases. Therefore, increasing of water percentage in the emulsion could decrease the stability of the pronounced nano-emulsion [33].

### 3.4. Interfacial tension and thermodynamic properties of used emulsifiers

Emulsion droplets are normally stabilized by surfactants or amphiphilic polymers. The adsorbed surfactant causes a lowering in interfacial tension for easier emulsification and stabilizes the droplet against coalescence by steric or electrostatic repulsion. Surfactants play a major role in the formation of nano-emulsion. The high energy required to form a nano-emulsion can be understood from a consideration of the Laplace pressure $P = 2\gamma/R$, where $R$ is the average radius of curvature of spherical emulsion drop. To break up a drop into smaller ones, it must be strongly deformed and must overcome the Laplace pressure $P$. Various processes can occur during emulsification, such as break up of droplet, adsorption of surfactants and droplet collision, which may or may not lead to coalescence of droplets [34].

The interfacial tension is directly related to the amount of stabilizer adsorbed and the nature of the interfacial layer [35]. Generally, the IFT depends on the type of emulsifier used to stabilize the water/diesel oil nanoemulsion, for example, when the oil droplet contains sufficient concentration of the low polarity emulsifier, the interfacial at oil/water interface is high. In contrast, the interfacial tension was decreased with high polarity emulsifier [36]. But, the presence of more than one surfactant molecule at the interface leads to decrease of the IFT comparing with individual emulsifier.

The interfacial tension properties for span 80, emarol 85 and (SE) at 30 °C are listed in Table 3 and illustrated in Fig. 5. From these obtained data, it is obvious that the interfacial tension ($\gamma$) decreased from 16.83 and 13.62 $mNm^{-1}$ for Span 80 and Emarol 85, respectively to 11 $mNm^{-1}$ for SE. Accordingly, the lowering of $\gamma$ causes a reduction in the droplet size where the amount of surfactant needed to produce the smallest drop size depends on the concentration of surfactant on the bulk which determines the reduction in $\gamma$, as given by the Gibbs adsorption equation,

$$-d\gamma = RTd\ln a \quad (9)$$

where $R$ is the gas constant, $T$ is the absolute temperature and $\Gamma$ is the surface excess (number of moles adsorbed per unit area of the interface).

By inspection the data listed in Table 3, it was found that there is a relation between the surface active properties and the efficiency of emulsifiers used to stabilize the W/O nano-emulsion. This means that the maximum enrichment of the emulsifier molecules on the interface was exhibited with the emulsifier, which has the smallest $A_{min}$ Also, a reversible proportion between $A_{min}$ and $\Gamma_{max}$ is noticed in Fig. 6, where with a small $A_{min}$, the maximum $\Gamma_{max}$ should occurred.

The maximum $\Gamma_{max}$ was exhibited with the blend emulsifier (SE) because the maximum synergism should happen with the mixture components, the result of a good emulsification and emulsion stabilization result was obtained. The individual demulsifier Span 80 exhibited a lower $A_{min}$ and higher $\Gamma_{max}$ among the emarol 85 and SE emulsifiers. These results of surface active properties for those emulsifiers consist of emulsion stability for them. Based on this, the use of SE will strongly adsorb to diesel droplets and, therefore, stabilize against coalescence in comparing with the use of span 80 or emarol 85 individually.

The results of the thermodynamic parameters of adsorption are shown in Table 3 for the same emulsifiers and gave evidence on the relation between the surface active proportions and the emulsification efficiency. The more $-\Delta G_{ad}$ value, indicates that the emulsifier molecules adsorbed strongly on the interface. Generally, the $-\Delta G_{ad}$ is slightly greater than $-\Delta G_{mic}$, which mean that the molecules prefer to adsorb on the interface than to make micelles. Therefore, the maximum $-\Delta G_{ad}$ (−17.18 KJ/mol) that was obtained with SE exhibited the maximum emulsification efficiency, while $-\Delta G_{ad}$ of emarol 85 (−21.83 KJ/mol) is smaller than span 80 (−18.63 KJ/mol). This means that the emarol 85 was adsorbed on the o/w interface and provide protection against coalescence comparing with span 80.

By comparing the data obtained from interfacial tension properties and thermodynamic parameters (see Table 3) with stability data of the nano-emulsions (Figs. 1 and 2), it was found that, there is a direct relationship between a reduction of ($\gamma$) and that obtained of the smallest droplet size. This means that, the droplet radius decreases with the increase the surfactant concentration and the decrease in interfacial tension ($\gamma$) of SE.

### 3.5. TEM image

The TEM image for the prepared nano-emulsion at 8% surfactant concentration, 10% water content, HLB = 10, after 360 h

**Table 3** Interfacial tension and thermodynamic properties for emulsifiers at 30 °C.

| Emulsifier | CMC (mol $dm^{-3}$) | $\gamma_{IFT}$ (mN/m) | $\Gamma_{max}$ ($10^{11}$ mol/$cm^{-2}$) | $A_{min}$ ($nm^2$) | $\pi$ (mN/m) | $\Delta G_{mic}$ (kJ /mol) | $\Delta G_{ad}$ (kJ /mol) |
|---|---|---|---|---|---|---|---|
| Span 80 | $1.82 \times 10^{-4}$ | 17.13 | 2.03 | 81.71 | 59.23 | −21.33 | −18.63 |
| Emarol 85 | $4.25 \times 10^{-5}$ | 12.77 | 1.91 | 86.89 | 54.87 | −24.93 | −21.83 |
| SE | $4.75 \times 10^{-4}$ | 10.85 | 3.44 | 48.16 | 61.15 | −18.96 | −17.18 |

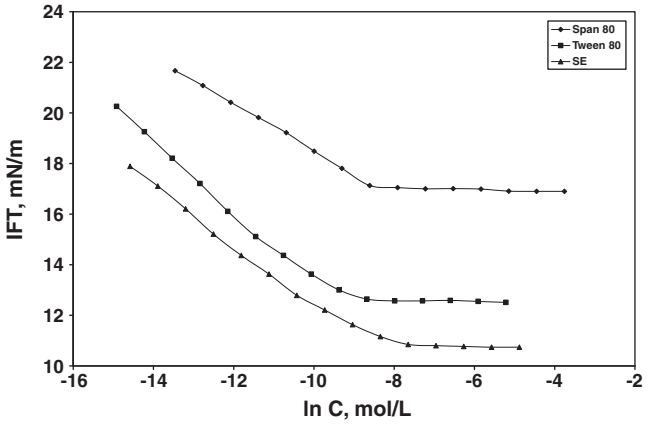


**Figure 5** Interfacial tension versus log C for water/emulsifiers/diesel oil system at 30 °C.

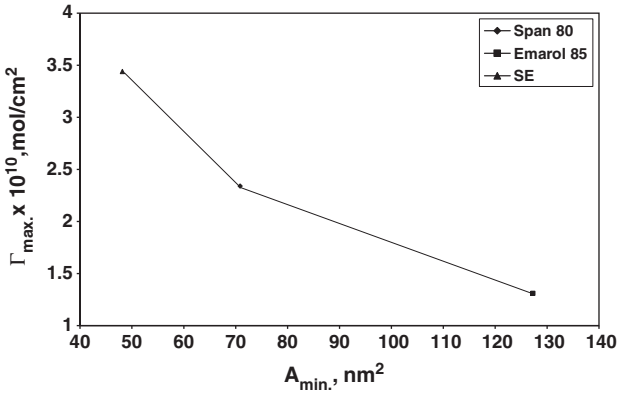


**Figure 6** Relation between $A_{min}$ against $\Gamma_{max}$ for water/emulsifiers/diesel oil system at 30 °C.

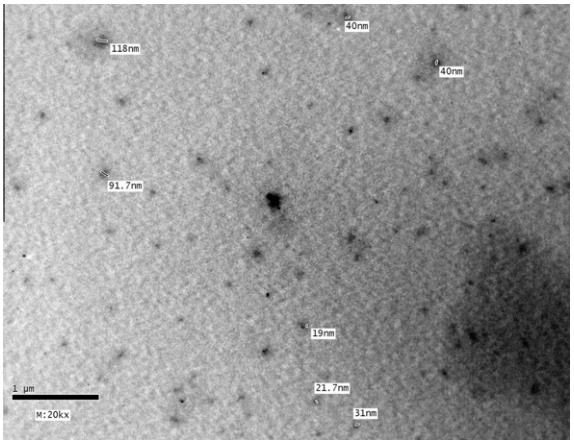


**Figure 7** TEM image water/SE/diesel oil at 8% surfactant concentration, 10% water content, HLB = 10 °C and 30 °C after 360 h.

and 30 °C is shown in Fig. 7. This figure shows the formation of transparent nano-emulsion with average spherical particle size equal to 80 nm. The water droplet in the nano-emulsion appears as a dark spherical shape, while the surrounding phase of diesel is shown as a bright phase. Accordingly, the radius of water droplet by TEM agreed with the data obtained by the dynamic light scattering.

## 4. Conclusion

The present results demonstrate the suitability of emulsifier blends to stabilize W/O nano-emulsion. The obtained nano-emulsions with a mean average particle size between 19.3 and 39 nm were influenced by the emulsifier concentration and water content. The stability of the studied emulsions increases with increasing total emulsifier concentration at low water content. Regarding interfacial tension and thermodynamic properties of the used emulsifiers, the individual emulsifiers span 80 and emarol 85 are not used as efficient emulsifiers but the blend emulsifiers (SE) between them in specific ratio with lowest interfacial tension is essential to obtaina very stable emulsion.

## References

[1] G.W. Lee, T.F. Tadros, Colloids and Surfaces 5 (1982) 105–115.
[2] H. Sagitani, In Organized Solutions, in: S.E. Friberg, B. Lindman (Eds.), Marcel Dekker, New York, 1992, pp. 259–271.
[3] A. Forgiarini, J. Esquena, C. Gonzalez, C. Solans, Langmuir 17 (7) (2001) 2076–2083.
[4] T.P. Hoar, J.H. Schulman, Nature 152 (1943) 102.
[5] E. Ruckenstein, J.C. Chi, Journal of the Chemical Society, Faraday Transactions 71 (1960) 2.
[6] J.T. Overbeek, Faraday Discussion of the Chemical Society 65 (1978) 7.
[7] D. Morales, J.M. Gutiérrez, M.J. Garcia, C. Solans, Langmuir 19 (2003) 7196.
[8] K. Shinoda, H. Saito, Journal of Colloid and Interface Science 26 (1968) 70.
[9] C. Solans, P. Izquierdo, J. Noll, N. Azemer, M.J. Garcia, Current Opinion in Colloid and Interface Science 10 (2005) 102–110.
[10] K. Landfester, M. Willert, M. Antonietti, Macromolecules 33 (7) (2000) 2370–2376.
[11] P. Fernandez, V. André, J. Riegger, A. Kühnle, Colloids and Surfaces A 251 (2004) 53–58.
[12] P. Izquierdo, J. Feng, J. Esquena, T.F. Tadros, J.C. Dederen, Journal of Colloid and Interface Science 285 (2005) 388–394.
[13] S. Kentish, T.J. Wooster, M. Ashokkumar, S. Balachandran, R. Mawson, L. Simons, Innovative Food Science and Emerging Technologies 9 (2008) 170–175.
[14] H.M. Courrier, T.F. Vandamme, M.P. Krafft, Colloid Surfaces A: Physicochemical and Engineering Aspects 244 (1–3) (2004) 141–148.
[15] F.F. Pischinger, Compression-ignition engines, in: E. Sher (Ed.) Handbook of Pollution from Internal Combustion Engines, London, UK, Academic Press, 1998, p. 261.
[16] C.Y. Lin, K.H. Wang, Fuel 18 (2) (2004) 477–484.
[17] A.Bertola, R. Li, K. Boulouchos, SAE paper tech. No. 2003-01-3146, 2003.
[18] G. Chen, D. Tao, Fuel Processing Technology 86 (2005) 499–508.
[19] A. AL-Sabagh, M. Nermine, E. Maysour, M.R. Noor El-Din, Journal of Dispersion Science and Technology 28 (2007) 547–555.
[20] R.A. Mohammed, A.I. Baily, P.F. Luckham, S.E. Taylor, Colloids and Surfaces Series A 83 (1994) 261–271.
[21] A.M. Al-Sabagh, M.M. Hamad, A.M. Badawi, N.E. Abdel-Moneem, Bull. Fac. Sci. Zagazig University 18 (2) (1996) 57–70.

[22] M.J. Rosen, Surfactants and Interfacial Phenomena, John Wily and Sons Inc., New York, USA, 1978.
[23] A.M. Al-Sabagh, Surface activity and thermodynamic properties of water-soluble polyester surfactants based on 1,3-dicarboxymethoxybenzene used for enhanced oil recovery, Polymers for Advanced Technologies 11 (2000) 48.
[24] L.L. Schramm, Surfactants: Fundamentals and Applications in Petroleum Industry, Cambridge University Press, Cambridge, England, 2000.
[25] J.W. Gibbs, The Collected Works of J. W. Gibbs Longman 1 (1928) 119.
[26] X. Liu, Y. Guan, Z. Ma, H. Liu, Longmuir 20 (2004) 10278.
[27] H.L. Wu, C. Ramachandran, N.D. Weiner, B.J. Rossler, International Journal of Pharmaceutics 220 (2001) 63.
[28] B. Deminiere, Modern Aspects of Emulsion Science, the Royal Society of Chemistry, in: B.P. Brnks (Ed.), Cambridge, UK, 1998, pp. 261–291.
[29] E.I. Taha, S. Al-Saidan, A.M. Samy, M.A. Khan, International Journal of Pharmaceutics 285 (2004) 109.
[30] W. Liu, D. Sun, C. Li, Q. Liu, J. Xu, Journal of Colloid and Interface Science 303 (2006) 557–563.
[31] S.H. Sajjadi, Chemical Engineering Science 61 (2006) 3009–3017.
[32] I. Capek, Advances in Colloid and Interface Science 107 (2003) 125.
[33] B.P. Binks, J.H. Clint, P.D.I. Fletcher, S. Rippon, Langmuir 15 (1999) 495.
[34] M. Porrasa, C. Solans, C. Gonzalez, A. Martınez, A. Guinart, J.M. Gutierrez, Colloids and Surfaces A: Physicochemical and Engineering Aspects 249 (2004) 115–118.
[35] G.W.J. Lee, Th.F. Tadros, Colloids and Surfaces 5 (1982) 105–115.
[36] I. Capek, Advances in Colloid and Interface Science 107 (2004) 125.